AMPA receptors associated with zebrafish Mauthner cells switch subunits during development

Shunmoogum Aroonassala Patten[1] and Declan W. Ali[1,2]

[1]*Department of Biological Sciences,* [2]*Centre for Neuroscience, Biological Sciences Building, University of Alberta, Edmonton, Alberta, Canada, T6G 2E9*

Glutamate AMPA receptors (AMPARs) are major excitatory receptors in the vertebrate CNS. In many biological systems there is a developmental speeding in AMPAR kinetics, which occurs either because of a switch in AMPAR subunits or a change in synaptic morphology. We studied the development of AMPAR-mediated miniature excitatory postsynaptic currents (AMPAR-mEPSCs) in zebrafish Mauthner cells (M-cells) to determine the reasons underlying the speeding of AMPA mEPSCs in this preparation. We recorded AMPAR-mEPSCs in zebrafish ranging in age from 33 h postfertilization (hpf) to 72 hpf. We found that the glutamate waveform in the synaptic cleft did not change during development, suggesting that synaptic morphology played little role in shaping the mEPSC. The current–voltage (I–V) relationship was linear at 33 hpf and outwardly rectified in older animals, while AMPAR decay kinetics were slower at positive potentials, compared with negative potentials. The relative change in τ with depolarization was found to be greater at 48 hpf than at 33 hpf. AMPARs in 33 hpf fish had a conductance of ∼9 pS, and in older fish ∼15 pS. Finally, the desensitization blocker, cyclothiazide, increased τ by ∼4-fold in 48 hpf preparations, but only 1.5-fold in 33 hpf fish. These results are consistent with the hypothesis that the major mechanism underlying the developmental speeding in AMPAR kinetics in zebrafish CNS is a switch in receptor subunits. To our knowledge this is the first study to suggest that AMPARs change subunits during development in fish.

(Received 6 February 2007; accepted after revision 3 April 2007; first published online 5 April 2007)
Corresponding author: Declan W Ali, Department of Biological Sciences and Centre for Neuroscience, Biological Sciences Building, University of Alberta, Edmonton, Alberta, Canada, T6G 2E9. Email: declan.ali@ualberta.ca

Fast excitatory synaptic transmission in the vertebrate CNS is mediated predominantly by the AMPA ionotropic glutamate receptor. AMPA receptors (AMPARs) govern the efficacy of synaptic transmission that is required for synaptogenesis, synaptic plasticity, and memory encoding (Schmitt *et al.* 2004; Vaithianathan *et al.* 2004). They are heteromultimeric structures comprised of glutamate receptor subunits 1–4 (GluR 1–4) with varying stoichiometries (Hollmann & Heinemann, 1994). AMPA receptors that contain GluR2 are impermeable to Ca^{2+} (Geiger *et al.* 1995; Seeburg, 1996; Cull-Candy *et al.* 2006), while receptors that lack this subunit are Ca^{2+} permeable. Further variation arises via alternative splicing to generate flip and flop forms of the subunits (Sommer *et al.* 1990).

The strength of synaptic transmission at excitatory synapses depends, in part, upon receptor properties such as channel conductance, open/close rates and burst behaviour (Ambros-Ingerson & Lynch, 1993; Benke *et al.* 1998; Lin *et al.* 2002). The amplitude and time course of the synaptic currents that are mediated by AMPARs are key players of synaptic information efficacy and cell excitability, and changes in the nature of these currents will impact upon cell activity. Developmental changes in the properties of synaptic currents have been observed at excitatory synapses (Sakmann & Brenner, 1978; Hestrin, 1992; Wall *et al.* 2002). However, information about developmental changes in AMPAR-mediated mEPSCs is somewhat contradictory. For example, in hippocampal pyramidal cells, AMPA receptor-mediated currents show an increase in decay times with maturation (Seifert *et al.* 2000), whereas other studies report a developmental decrease in decay time constants (Taschenberger & von Gersdorff, 2000; Iwasaki & Takahashi, 2001; Joshi & Wang, 2002; Wall *et al.* 2002; Yamashita *et al.* 2003; Rumpel *et al.* 2004). The time course of synaptic currents depends upon factors such as receptor affinity (Jones *et al.* 1998), desensitization (Jones & Westbrook, 1996), glutamate dynamics in the synaptic cleft (e.g. release, clearance) and synaptic morphology (Cathala *et al.* 2005). The two main mechanisms that are thought to primarily underlie the developmental speeding of AMPA mEPSCs

This paper has online supplemental material

 DOI: 10.1113/jphysiol.2007.129999

are (1) changes in receptor subunit composition (Lawrence & Trussell, 2000; Kumar *et al.* 2002); and (2) changes in synaptic morphology (Cathala *et al.* 2005). It is unknown if a developmental change in AMPAR kinetics occurs in zebrafish, and if so, what the underlying mechanism might be.

Mauthner cells (M-cells) are the largest neurons in the teleost's CNS and play key roles in escape behaviours (Kimmel *et al.* 1981; Metcalfe *et al.* 1990). The earliest synapses on M-cells are established by around 24 h postfertilization (hpf) (Kimmel *et al.* 1990), with functional inputs occurring around 26–27 hpf (Grunwald *et al.* 1988; Ali *et al.* 2000*b*). Some characteristics of GluRs on developing M-cells have already been investigated (Ali *et al.* 2000*a*), but the developmental profile of AMPAR properties is still to be determined. The zebrafish is an excellent preparation to study synaptic development, because the wide variety of locomotor mutants that are available and the recent sequencing of the genome allow a thorough genetic investigation into synaptic maturation. Furthermore, because Mauthner cells are involved in simple locomotor behaviours, such as the C-start reflex, the development of excitatory synapses associated with these cells can be related to behaviours in developing fish (Liu & Fetcho, 1999; Fetcho, 2006).

Therefore, we have undertaken this study to examine the developmental properties of AMPAR-mediated currents *in vivo*, on zebrafish M-cells. We show that there is indeed a developmental change in the AMPAR-mEPSC kinetics and that this change appears to be due to subunit switching rather than a change in synaptic morphology.

Methods

Preparation

Wild-type Zebrafish (*Danio rerio*) embryos were raised at 28.5°C, and collected and staged as previously described (Kimmel *et al.* 1995; Westerfield, 2000). All procedures were carried out in compliance with the guidelines stipulated by the Canadian Council for Animal Care and the University of Alberta. Embryos and newly hatched larvae were anaesthetized in 0.02% tricaine (MS-222) (Sigma, St Louis, MO, USA) and dissected as described by Drapeau *et al.* (1999). Briefly, the entire hindbrain was exposed after removing the forebrain and rostral structures, but leaving the spinal cord intact.

Electrophysiology

The preparations were moved to the recording set-up and the chamber was continuously perfused at room temperature (20–24°C) with an aerated recording solution that contained 15 μM D-tubocurarine (Sigma) to paralyse the preparations, but lacked tricaine. The recording solution contained (Evans, 1979) (mM): 134 NaCl, 2.9 KCl, 2.1 $CaCl_2$, 1.2 $MgCl_2$, 10 Hepes, and 10 glucose, osmolarity adjusted to 290 mosmol l^{-1}, pH 7.8. Whole-cell recordings were obtained from Mauthner neurons located in rhombomere 4. These cells were easily identified under Nomarski differential interference contrast (DIC) optics based on their morphology and location in the hindbrain (Fig. 1*A*; Eaton and Farley, 1973). Cells were filled with Lucifer Yellow (0.1%) to confirm their identity. Patch-clamp electrodes were pulled from borosilicate glass and when filled with a Cs-gluconate solution had resistances of 3.5–5 MΩ. The Cs-gluconate intracellular solution was composed of (mM) 115 Cs-gluconate, 15 CsCl, 2 $MgCl_2$, 10 Hepes, 10 EGTA, and 4 Na_2ATP, osmolarity adjusted to 280 mosmol l^{-1}, pH 7.2.

Whole-cell currents were recorded using an Axopatch 200B amplifier (Axon Instruments) and were low-pass filtered at 10 kHz (−3 dB) and digitized at 40–50 kHz. Synaptic currents were recorded at a holding potential of −60 mV unless otherwise noted. All events were recorded in the presence of strychnine (5 μm), picrotoxin (100 μm), APV (50 μm) and TTX (1 μm) to isolate AMPA mEPSCs at all holding potentials. Immediately after establishment of the whole-cell recording mode, series resistance was compensated by 60–85%, using the amplifier's compensation circuitry. To determine current–voltage (I–V) relationships, mEPSC recordings were performed at a series of membrane command potentials ranging from −80 mV to +80 mV. The potential was stepped to a new constant value before the start of sampling (2–4 s) in order to allow the membrane current to relax to a plateau level. The mean (± S.E.M.) series resistance was 9 ± 3 MΩ, and recordings in which the series resistance changed by at least 15% or membrane potentials were more positive than −45 mV were discarded. The liquid junction potential between the pipette and external solution was not corrected for.

Analysis of mEPSCs

Synaptic activity was monitored using pClamp 8.1 software (Axon Instruments). Synaptic events were detected (using the template function for events >2.5 standard deviations above the basal noise) and analysed with Axograph 4.6 (Axon Instruments). The software detected all events that could be recognized visually. All events were then inspected visually, and those with uneven baselines or overlaying events (<5%) were discarded. The decay time course was analysed over the first 30 ms for pure AMPA events and was fitted with a sum of exponential curves. The presence of one or two exponential components during the decay of the mEPSCs was tested by comparing the sum of squared errors of the fits over the same decay ranges (Clements & Westbrook, 1991; Legendre, 1998). Averages of these events were always best fitted with one exponential curve. The rise

times were defined as the time from 20% to 80% of the mEPSC amplitude. All data values are given as means ± S.E.M. Correlations were calculated with the use of a least-squares linear regression analysis. Significance was determined using one-way ANOVAs and Fisher LSD tests for normally distributed, equal variance data and paired *t* tests. Kruskal–Wallis ANOVA and Dunn's method of comparison were used for non-normal distributions. * denotes $P < 0.05$ and ** denotes $P < 0.01$.

Non-stationary fluctuation analysis

We performed non-stationary fluctuation analysis to estimate the single-channel current (i) and the available number of channels (N) (NSFA; Sigworth, 1980). The mEPSCs were aligned on their rise times, and events with obvious artifacts were manually discarded. Non-stationary analysis was performed on the deactivation phase of the responses. The averaged current and variance over time were computerized using Axograph 4.6 software after digital filtering of the traces at 2 kHz. Between 20 and 80 traces per patch were obtained for analysis.

The variance (σ^2) was plotted against the mean current (I) and the data points were fitted with the following parabolic function (Sigworth, 1980):

$$\sigma^2(I) = iI - I^2/N + \sigma_b^2$$

where i is the elementary current of the receptor channel, N is the total number of available AMPARs at the synapse and $\sigma_b{}^2$ is the variance of the background noise. A linear fit to the initial part of the curve (10–15% of the response range) yields a slope factor that corresponds to the single-channel current (i) (Benke *et al.* 2001). All estimates for which the initial rising phase of the current-variance plot was well-fitted by a linear fit, produced similar values for conductance (γ), as previously reported (Traynelis *et al.* 1993; Benke *et al.* 1998). The slope conductance value (γ) for each channel was then calculated by the equation $\gamma = i/(V_m - E_{rev})$, with $V_m = -60$ mV and $E_{rev} = 0$ mV.

Chemicals

All drugs were dissolved in the aerated recording solution and applied by bath perfusion. Strychnine (5 μM), picrotoxin (100 μM), CNQX (10 μM), APV (50 μM), cyclothiazide (CTZ; 10 μM), kynurenic acid (KYN; 50 μM), SYM (10 μM) and GYKI (50 μM) were obtained from Sigma. Tetrodotoxin (TTX; 1 μM) and DL-TBOA (100 μM) were purchased from Tocris (Avonmouth, UK).

Results

In this study, we examined the properties of AMPAR-mediated currents in M-cells of zebrafish ranging in age from 30 hpf to 72 hpf. Recordings were limited to these ages due to the difficulty of obtaining sufficiently clean dissections before 30 hpf, and the difficulty of recording from large, improperly clamped M-cells in animals older than 72 hpf. Recordings taken from 30 hpf to 36 hpf fish were pooled and are referred to as 33 hpf throughout the study. Recordings taken at 2 days post-fertilization were more accurately staged as 48 ± 3 hpf, while recordings at 3 days of age were 72 ± 3 hpf. In the remainder of the study these periods are referred to as 48 hpf and 72 hpf respectively. The cell capacitance (C_m) values ranged from 17 ± 2 pF (33 hpf) to 28 ± 1 pF in 48 hpf fish, and finally to 32 ± 2 pF in 72 hpf fish. Values for the membrane resistance (R_m) were 902 ± 36 MΩ (33 hpf), 253 ± 48 MΩ (48 hpf) and 87 ± 19 MΩ (72 hpf), while the resting membrane potentials were −54 ± 1 mV (33 hpf), −58 ± 2 mV (48 hpf) and −61 ± 2 mV (72 hpf).

Isolation of non-NMDA-mediated mEPSCs

We identified M-cells *in vivo* based upon the location of their large cell bodies adjacent to the otic vesicles in the hindbrain. Cells were filled with Lucifer yellow to confirm their identity (Fig. 1*A*).

Miniature EPSCs, unlike evoked currents, allow accuracy in determining the properties of postsynaptic receptors because their decay kinetics in particular can be highly influenced by developmental changes in the synchrony of vesicular release or release probability (Silver *et al.* 1996; Wall *et al.* 2002; Cathala *et al.* 2005). Therefore, we focused our analysis on mEPSCs to determine the developmental changes in the properties of postsynaptic receptors.

A high level of synaptic activity was observed when we recorded from the M-cells in normal physiological saline (Fig. 1*B*). The M-cells were clamped at a holding potential of −60 mV, where all inhibitory currents were small and inward. To differentiate inward, excitatory currents from inhibitory currents, blockers for glycine and GABA receptors (5 μM strychnine and 100 μM picrotoxin, respectively) were added to the bath during all recordings. In these initial experiments, 50 μM APV was added to the bath to block all NMDA receptor activity (Fig. 1*C*), but we found that isolated non-NMDA mEPSCs were identical in all aspects when recorded in the presence or absence of APV. Therefore we omitted APV for all further recordings at −60 mV, but included it when recording at potentials more positive than −60 mV. Miniature EPSCs were recorded in the presence of 1 μM TTX (Fig. 1*C*). The remaining mEPSCs were completely blocked by the non-NMDA antagonist CNQX (10 μM; Fig. 1*C*). Individual mEPSCs from a recording were averaged, and all analyses were performed on averaged mEPSCs (Fig. 1*D*).

Developmental profile of non-NMDA mEPSCs

Because it is difficult to properly clamp cells with large and extensive dendrites, whole-cell recordings are often subject to the problem of inadequate space clamp (Rall, 1969). Accurate control of dendritic potentials from a point voltage source is difficult, and synaptic events that are generated at more distal locations may be filtered leading to attenuation and widening. Thus, these events will appear to have longer rise times, smaller peak amplitudes and longer decays (Rall, 1969). Therefore, the correlation between the rise time and peak amplitude of events at 33 hpf, 48 hpf and 72 hpf (Fig. 2*A*) were examined for all recordings to determine if cells were properly space clamped. The lack of a correlation at all ages ($r = 0.02$ at 33 hpf; $r < 0.01$ at 48 hpf; $r = 0.04$ at 72 hpf), suggests that the M-cells remained electrically compact over the ages examined, and that space-clamping errors were not a major issue

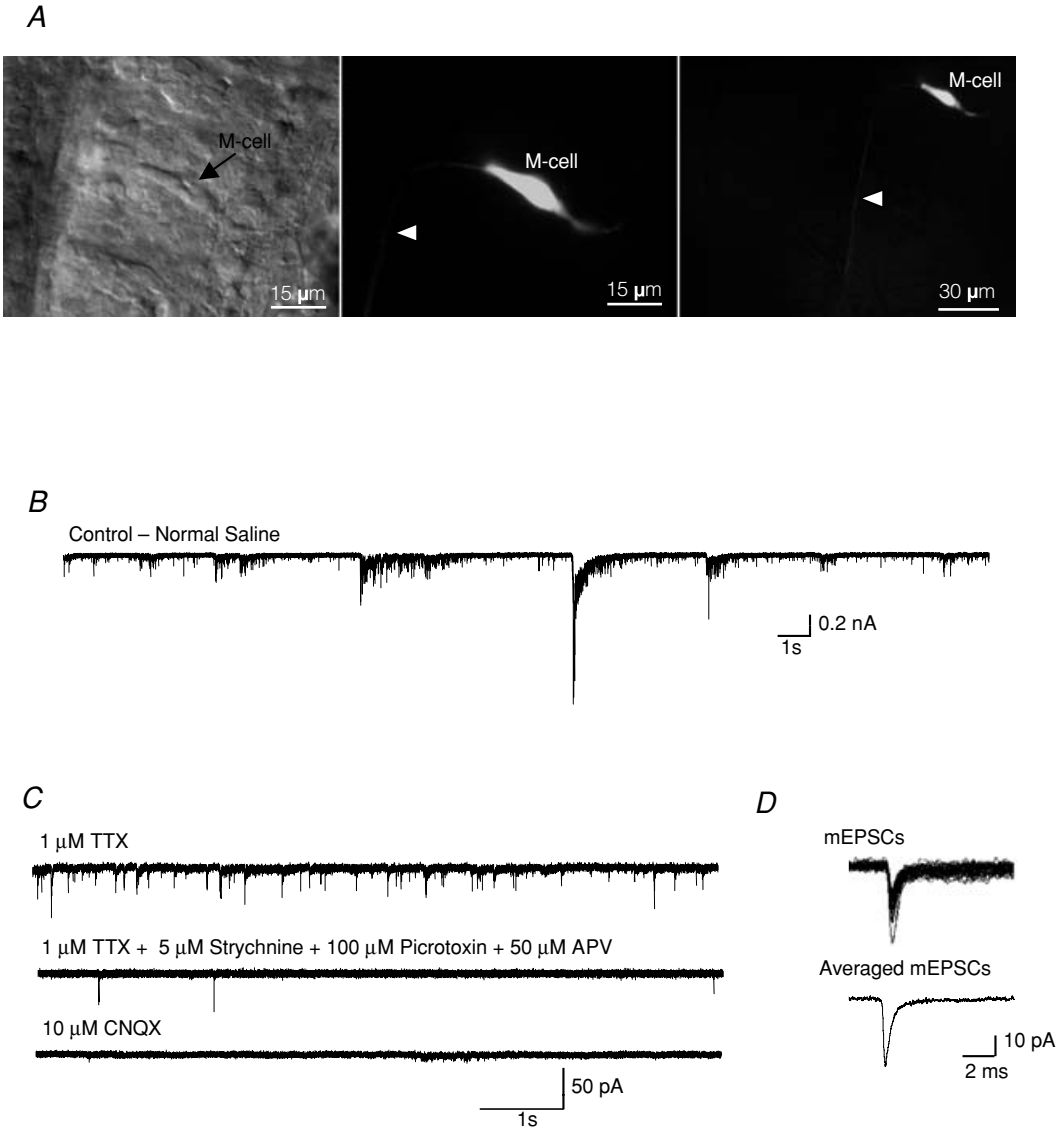

Figure 1. Spontaneous synaptic activity in Mauthner cells (M-cells)
A, differential interference contrast image of an M-cell in a hindbrain preparation. Arrow points to the cell body (left panel). The same M-cell was filled with Lucifer Yellow (0.1%) during a typical experiment (middle and right panel). Arrowhead points to the axon descending into the spinal cord. Scale bar: 15 μm in the left panel and the middle panel, and 30 μm in the right panel. *B*, spontaneous activity in an M-cell recorded in normal extracellular saline solution. *C*, miniature postsynaptic currents (mEPSCs) recorded in the presence of 1 μM TTX, 5 μM strychnine, 100 μM picrotoxin and 50 μM APV. All mEPSCs were completely blocked after bath application of the non-NMDA receptor antagonist CNQX (10 μM). *D*, individual mEPSCs were acquired (top) and averaged (bottom). Holding potential was −60 mV.

in our study. The mEPSC amplitude distribution at all ages remained unimodal (Fig. 2*B*), with the average peak amplitude increasing significantly between 33 hpf and 48 hpf (33 hpf: 23.9 ± 2.0, $n = 10$; 48 hpf: 30.0 ± 1.5, $n = 9$ and 72 hpf: 29.4 ± 0.9, $n = 8$; $P < 0.05$) (Fig. 2*B*). Amplitude histograms from representative experiments are shown in Fig. 2*C*. The tight, normal distributions suggest that there was very little or no variation in quantal size.

We observed a significant increase in the mEPSC frequency during development, from 0.7 ± 0.3 Hz in 33 hpf embryos to 2.8 ± 0.4 Hz in 72 hpf larva (Fig. 3*A*; $P < 0.05$). mEPSC frequency was more variable in the 48 hpf larvae (3.1 ± 0.7 Hz) compared with the 33 hpf and 72 hpf animals, suggesting that it is within this transition period that new synapses are forming or existing synapses are becoming more active.

The rise times, defined as the time from 20% to 80% of the mEPSC amplitude, were fast, averaging 0.13 ± 0.02 ms at 33 hpf, 0.11 ± 0.01 ms at 48 hpf and 0.11 ± 0.01 ms at 72 hpf, and were not significantly different over the developmental stages examined (Fig. 3*B*). Average mEPSC traces were well fitted with a single exponential decay curve, which decreased during development. The decay kinetics were significantly slower at 33 hpf (0.75 ± 0.09 ms) when compared with those of older animals (48 hpf: 0.47 ± 0.03 ms and 72 hpf: 0.48 ± 0.02) (Fig. 3*C* and *D*; $P < 0.01$). This finding is consistent with other studies that demonstrate a speeding in the time course of AMPAR-mediated EPSCs during CNS

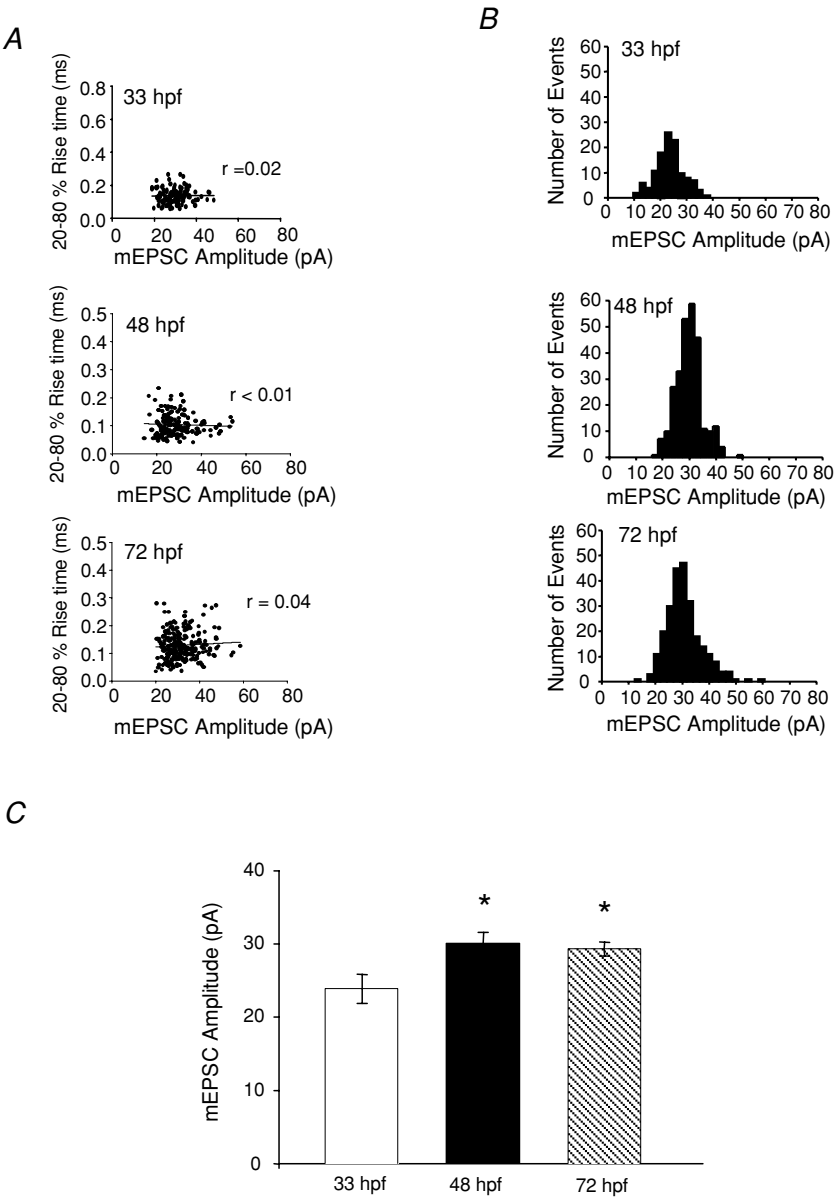

Figure 2. Isolated non-NMDA mEPSCs from M-cells are properly space clamped
A, scatter plots of rise time *versus* amplitude of events recorded from a 33 hpf preparation($r = 0.02$; $n = 158$ events), 48 hpf preparation ($r < 0.01$; $n = 218$ events), and a 72 hpf preparation ($r = 0.04$; $n = 249$ events). *B*, amplitude histogram of mEPSCs from an M-cell recorded at 33 hpf, 48 hpf and 72 hpf in the presence of 1 μM TTX, 5 μM strychnine, 100 μM picrotoxin (bin width = 2 pA; $n = 109$ (33 hpf); $n = 278$ (48 hpf); $n = 251$ (72 hpf)). *C*, peak amplitude of non-NMDA mEPSCs recorded in the presence of 1 μM TTX, 5 μM strychnine, and 100 μM picrotoxin. (33 hpf: 24 ± 2.0 pA, $n = 10$ embryos; 48 hpf: 30 ± 2 pA, $n = 9$ larvae and 72 hpf: 30 ± 1 pA, $n = 8$ larvae). *C*, holding potential was −60 mV. *Significantly different from 33 hpf, $P < 0.05$. Error bars represent S.E.M.

maturation (Bellingham *et al.* 1998; Taschenberger & von Gersdorff, 2000; Brenowitz & Trussell, 2001; Kumar *et al.* 2002; Wall *et al.* 2002; Cathala *et al.* 2003).

mEPSCs are mediated solely by AMPARs

To determine if the mEPSCs were mediated by AMPA or kainate receptors, we examined the effect of the selective AMPAR antagonist (GYKI; 50 μM), and the selective kainite-desensitizing agent SYM (10 μM) on mEPSCs. We found that GYKI completely blocked all mEPSCs and that SYM had no effect on either the mEPSC frequency, amplitude, rise time or the decay time constant ($P > 0.05$; see Fig. 1 in online Supplemental material). These results suggest that the mEPSCs were due solely to the activation of AMPA receptors and lacked a kainate component at all ages.

The marked change in postsynaptic currents during development depends on a number of factors (Edmonds *et al.* 1995; Conti & Weinberg, 1999), most notably a change in synaptic morphology (Cathala *et al.* 2005) or a switch in receptor subunits (Kumar *et al.* 2002; Wall *et al.* 2002). Therefore, we next investigated the mechanism underlying the developmental changes observed in the AMPAR-mediated mEPSC kinetics between 33 hpf and 48 hpf.

Effect of glutamate uptake in shaping the mEPSC

The glutamate transient in the synaptic cleft changes shape due to alterations in synaptic morphology that might occur during development (Lee & Sheng, 2000). These changes have been shown to lead to faster glutamate clearance from the cleft (Otis *et al.* 1996; Diamond & Jahr, 1997), resulting in a shorter mEPSC decay time constant. Therefore it was possible that the developmental decrease in τ that we had noted was due to faster clearance of glutamate from the cleft. To test this, we recorded AMPAR-mEPSCs in the presence and absence of the glutamate transporter blocker DL-TBOA. Our rationale was that if the faster events in older animals were due to the appearance of glutamate transporters, then DL-TBOA should block their activity and widen the mEPSC in older animals (48 hpf) compared with younger ones (33 hpf). However, we found that DL-TBOA did not affect the mEPSC frequency, amplitude, rise time and decay time constant at any age ($P > 0.05$; see Fig. 2 in online Supplemental material). The lack of effect of DL-TBOA indicates that glutamate uptake does not play a major role in shaping the AMPAR-mESPC in zebrafish.

Additionally, developmental changes in AMPAR-mEPSC kinetics might be due to an increased concentration of glutamate in the synaptic cleft. The glutamate receptor antagonist kynurenic acid (KYN) may be used to detect changes in the glutamate concentration in the synaptic cleft because the effect of KYN would be weaker if the glutamate concentration in the synaptic cleft is higher (Diamond & Jahr, 1997; Wadiche & Jahr, 2001; Yamashita *et al.* 2003). Application of KYN resulted in a reduction in the mEPSC peak amplitude (Fig. 4*C*) at both 33 hpf and 48 hpf as expected; however, the reductions were to similar extents (Fig. 4*D*; $P > 0.05$) suggesting that the glutamate concentration in the synaptic cleft does not change significantly during development.

Since our results indicated that changes in the glutamate transient do not contribute to the changes in AMPAR-mEPSC kinetics during M-cell maturation, we next investigated whether these developmental changes in the AMPAR-mEPSC kinetics were due to alterations in postsynaptic receptor properties.

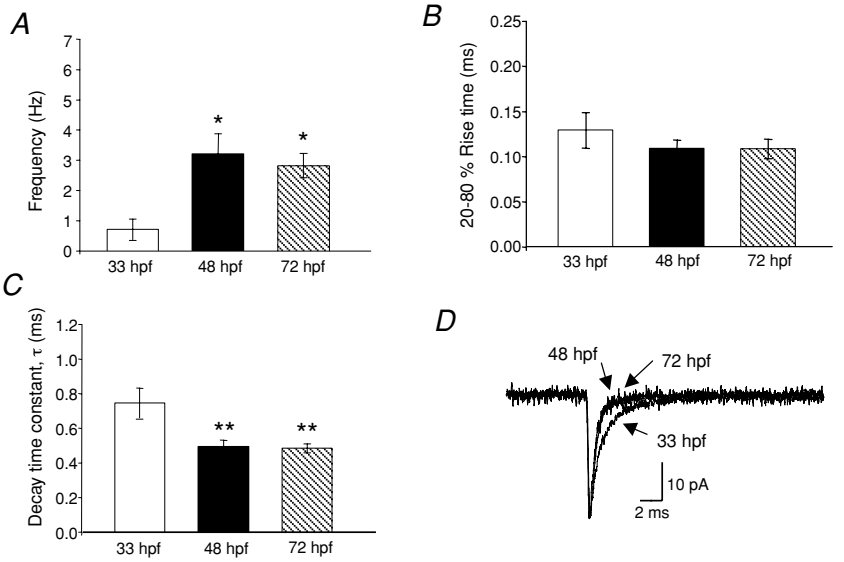

Figure 3. Frequency, rise time and decay kinetics of non-NMDA mEPSCs
A, frequency bar graph of the mEPSCs recorded at different ages. *B*, 20–80% rise time was 0.13 ± 0.02 ms at 33 hpf ($n = 10$ embryos); 0.11 ± 0.01 ms at 48 hpf ($n = 9$ larvae) and 0.11 ± 0.01 ms at 72 hpf ($n = 8$ larvae). *C*, bar graph of the decay time constant which was fitted with a single exponential function. τ was 0.75 ± 0.09 ms at 33 hpf ($n = 10$ embryos), 0.50 ± 0.03 ms at 48 hpf ($n = 9$ larvae) and 0.49 ± 0.03 ms at 72 hpf ($n = 8$ larvae). *D*, superimposed averaged mEPSC at 33 hpf, 48 hpf and 72 hpf. Note the slower decay at 33 hpf. The holding potential was −60 mV
*Significantly different from 33 hpf $P < 0.05$; **significantly different from 33 hpf $P < 0.01$.

Voltage dependence of AMPAR-mediated mEPSCs

Because the *I–V* relationship of AMPARs is known to be subunit dependent (Geiger *et al.* 1995; Sah & Lopez De Armentia, 2003), we examined the voltage dependence of the mEPSCs by varying the membrane holding potential in steps of 20 mV increments from −80 mV to +80 mV. In order to analyse the current–voltage (*I–V*) relationship quantitatively, we averaged well-isolated AMPAR-mEPSCs occurring during 30–60 s time periods ($n = 4$–9) at each holding potential, and plotted the peak amplitude of each averaged mEPSC against the holding potential (Fig. 5*A* and *B*). We found that the *I–V* relationship at 33 hpf was linear (Fig. 5*A*), while at 48 hpf, it displayed outward rectification. The *I–V* relationship at 72 hpf also exhibited outward rectification (data not shown), similar to that at 48 hpf. Even though our outward rectification *I–V* relationship is similar to that observed in cells in the nucleus magnocellularis (Otis *et al.* 1995), outward rectification is rare for AMPA receptors and most cells containing AMPAR receptors show a linear or inwardly rectifying *I–V* relationship.

Notably, we found that the time course of the decay phase of the mEPSC was voltage dependent, with a slower decay at more positive potentials. When cells were depolarized from −60 mV to +80 mV, the 33 hpf decay time constant increased from 0.76 ± 0.06 to 0.95 ± 0.05 ms ($n = 4$), which represents an increase of $20 \pm 3\%$. The 48 hpf decay time constant increased by a much larger percentage, from 0.49 ± 0.07 ms to 1.1 ± 0.05 ms ($n = 4$), representing an increase of $55 \pm 5\%$ (Fig. 6*A* and *B*; $P = 0.004$). These differences suggest that the receptors themselves may be different. To confirm that the EPSC decay kinetics were not affected by dendritic

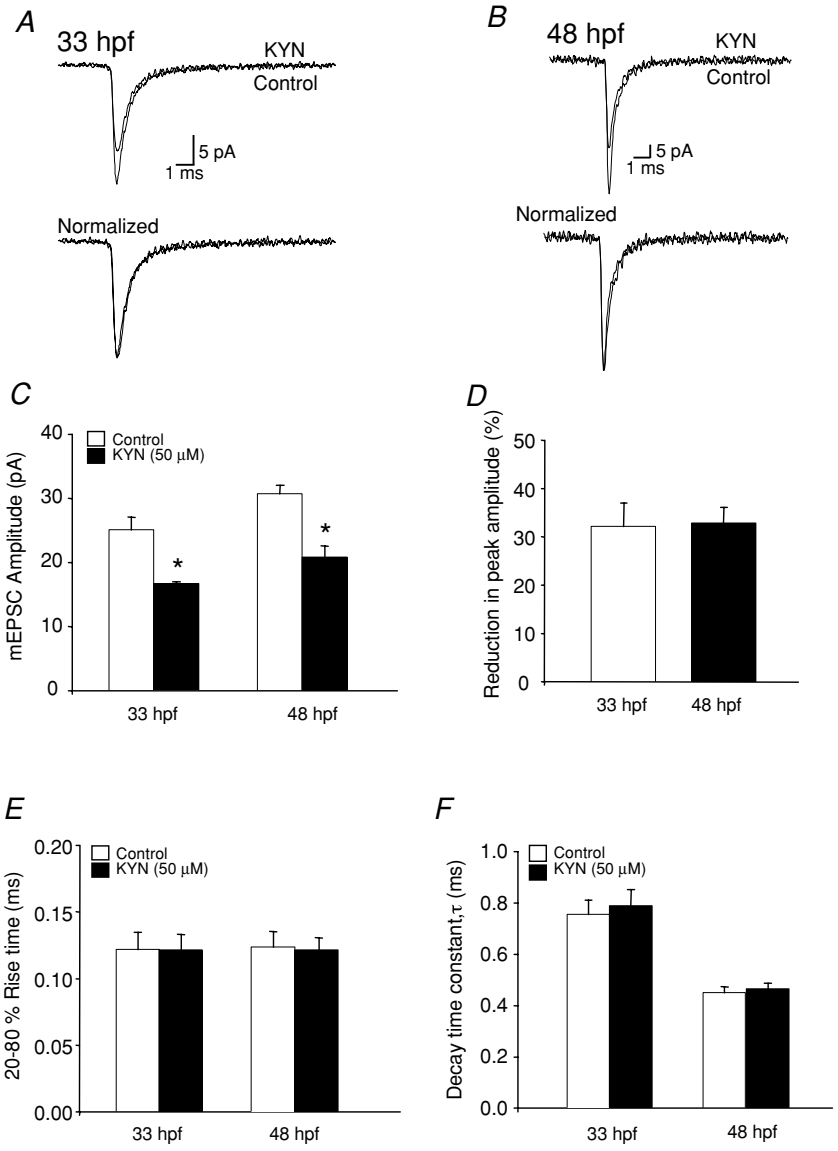

Figure 4. Effect of the glutamate receptor antagonist kynurenic acid (KYN) on AMPAR-mEPSC
A, superimposed (top) and normalized (bottom) mEPSCs recorded from 33 hpf M-cells in the absence and presence of 50 μM KYN ($n = 4$ embryos) *B*, superimposed (top) and normalized (bottom) mEPSCs recorded from 48 hpf M-cells in the absence (control) and presence of 50 μM KYN ($n = 5$ larvae). *C*, mEPSC peak amplitude recorded in the absence (control, open bars) and presence (filled bars) of 50 μM KYN at 33 hpf ($n = 4$ embryos) and 48 hpf ($n = 5$ larvae). *D*, bar graph showing percentage inhibition of peak amplitude induced by 50 μM KYN at 33 hpf and 48 hpf. *E*, 20–80% rise time bar graph of the mEPSCs recorded in the absence (control, open bars) and presence (filled bars) of 50 μM KYN at 33 hpf ($n = 4$ embryos) and 48 hpf ($n = 5$ larvae). *F*, bar graph of the decay time constant, τ, at 33 hpf ($n = 4$ embryos) and 48 hpf ($n = 5$ larvae) recorded in the absence (control, open bars) and presence (filled bars) of 50 μM KYN. *Significantly different from control, $P < 0.05$.

filtering when the cells were clamped at positive potentials; we analysed the change in rise time with depolarization at both age groups. The mEPSC rise time did not change in depolarized cells at either age (Fig. 6*C*), suggesting that at positive potentials the M-cells were indeed properly clamped.

Estimates of synaptic channel conductance

Because our data suggested that the receptors at the two ages may indeed be different, we determined the single-channel conductance of the AMPARs at 33 hpf and 48 hpf. In order to do this, we performed non-stationary fluctuation analysis (NSFA) on AMPAR-mEPSCs. Estimates of AMPAR unitary conductance (γ) and numbers of active channels (N) can be obtained from analyses of miniature synaptic events, which examine the variance of fluctuations in the decay phase of synaptic events (Traynelis *et al.* 1993; Benke *et al.* 1998). This analysis is based on the assumption that the opening and closing of individual channels are independent events. Thus, the event-to-event fluctuations in synaptic currents will be smallest at the peak and end portion of the event, and largest during the decay phase, as determined by single-channel conductance and the number of functional channels. Variance–current plots were constructed at both ages, and estimates of γ and N were derived from fitted functions (see Methods). We found a significant difference in γ between the two ages (33 hpf: 9.6 ± 0.52 pS and 48 hpf: 15.2 ± 1.17 pS; $n = 6$; $P = 0.002$; Fig. 7), suggesting that the AMPARs at 33 hpf and at 48 hpf are truly different. There was no significant change in the number of active channels during development. Specifically, we found that at 33 hpf the number of active channels was 28 ± 2 and at 48 hpf, it was 33 ± 5 ($n = 5$ at 33 hpf and $n = 6$ at 48 hpf; $P = 0.38$).

Cyclothiazide modulation of AMPAR-mEPSCs kinetics

Lastly, we examined the effect of cyclothiazide (CTZ) on AMPA mEPSCs. CTZ suppresses the desensitization of AMPA receptors (Partin *et al.* 1993; Wong & Mayer, 1993), but does so to a greater degree on the flip splice variants and on heteromeric receptors (Partin *et al.* 1994, 1995; Cotton & Partin, 2000). Therefore, differential effects of CTZ imply the presence of different subunits, which may underlie the speeding of the AMPAR kinetics in older animals. We used a low concentration (10 μM) of CTZ to discern between flip and flop forms of the subunits (Partin *et al.* 1994; Cathala *et al.* 2005). We found that CTZ had no effect on the mEPSC frequency, amplitude or rise time ($P > 0.05$ Fig. 8*C*); however, the decay time at both ages was significantly increased (33 hpf, $P = 0.011$; 48 hpf $P = 0.012$; paired t tests). The decay time constant in 33 hpf controls was 0.8 ± 0.07 ms and increased to 1.2 ± 0.1 ms ($n = 3$) in the presence of CTZ, and in 48 hpf controls was 0.5 ± 0.03 ms and increased to 2.1 ± 0.2 ms ($n = 4$) in the presence of CTZ. Therefore, CTZ showed a stronger potentiation of the decay time constant in the older animals (a 4-fold increase in τ at 48 hpf) compared

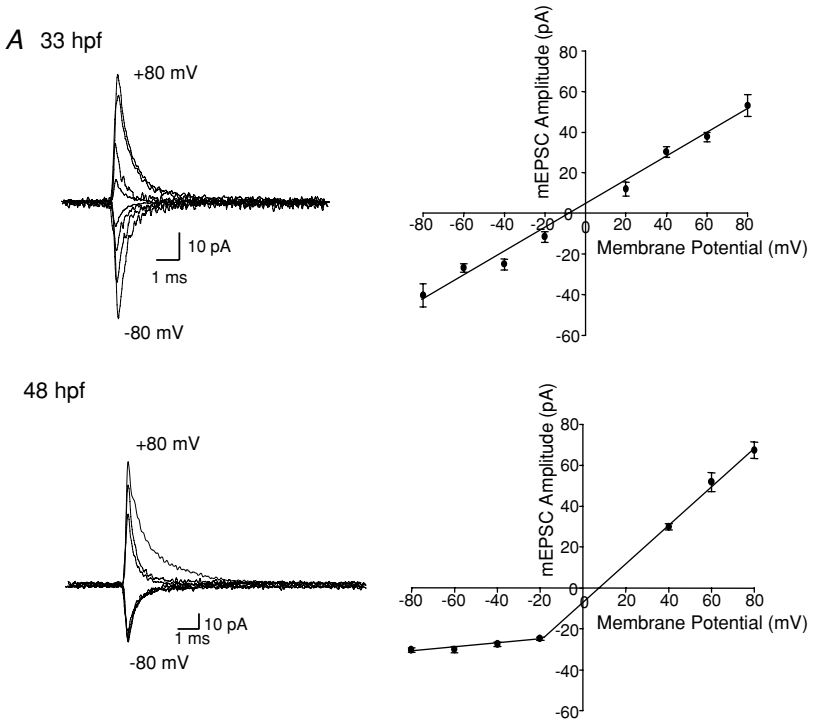

Figure 5. Voltage dependence of AMPAR-mEPSCs
All events were recorded in the presence of strychnine (5 μm), picrotoxin (100 μm), APV (50 μm) and TTX (1 μm) to isolate AMPA mEPSCs at all holding potentials. *A*, *I–V* relationship of averaged mEPSCs at 33 hpf ($n = 4$–10 embryos) at different holding potentials ranging from −80 mV to +80 mV in 20 mV increments; right *I–V* plot of pooled data was linear *B*, averaged mEPSC *I–V* relationship at 48 hpf ($n = 4$–9 larvae); right *I–V* plot of pooled data at different holding potentials from −80 mV to +80 mV, was outwardly rectified. AMPA mEPSCs at +20 mV in 48 hpf fish are omitted because they were small in amplitude and were difficult to isolate above background noise.

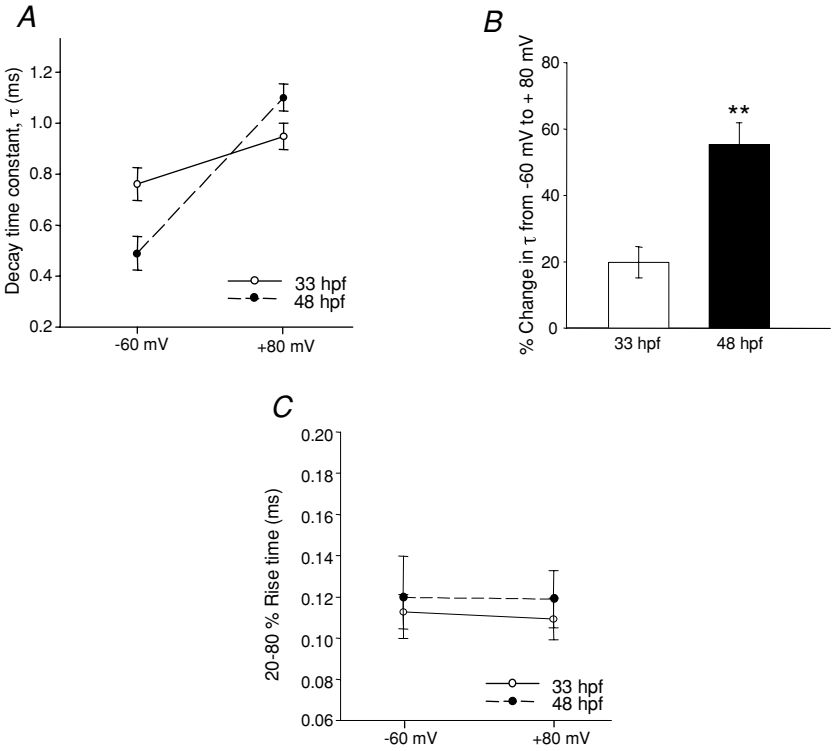

Figure 6. Voltage dependence of AMPAR-mEPSC decay time constant
All events were recorded in the presence of strychnine (5 μm), picrotoxin (100 μm), APV (50 μm) and TTX (1 μm) to isolate AMPA mEPSCs at all holding potentials. *A*, plot of mEPSC decay time constant at −60 mV and +80 mV at 33 hpf ($n = 4$ embryos, ○ and continuous line) and at 48 hpf ($n = 4$ larvae, ● and dashed line). *B*, bar graph showing the percentage change in τ from −60 mV to +80 mV. *C*, plot of 20–80% rise time at −60 mV and +80 mV. *Significance at $P < 0.05$ and ** at $P < 0.01$.

with the younger ones (1.5-fold increase in τ at 33 hpf; Fig. 8*D*; $P = 0.025$, ANOVA). These observations suggest that AMPARs at 33 hpf are composed of subunits that are different from those at 48 hpf.

Discussion

The present results suggest that AMPAR-mediated currents on Mauthner neurons change properties during development due to the expression of different receptor subtypes. Recent findings of AMPA-EPSCs in cerebellar granule cells suggested that developmental alterations in the kinetics of AMPAR-mediated currents occur because of changes in synaptic morphology (Cathala *et al.* 2005) rather than differential subunit assembly, as shown in other systems (Lawrence & Trussel, 2000; Kumar *et al.* 2002). These intriguing findings prompted us to investigate whether or not similar changes occur in AMPAR-mediated currents on zebrafish M-cells. Here we show that the developmental changes in the properties of

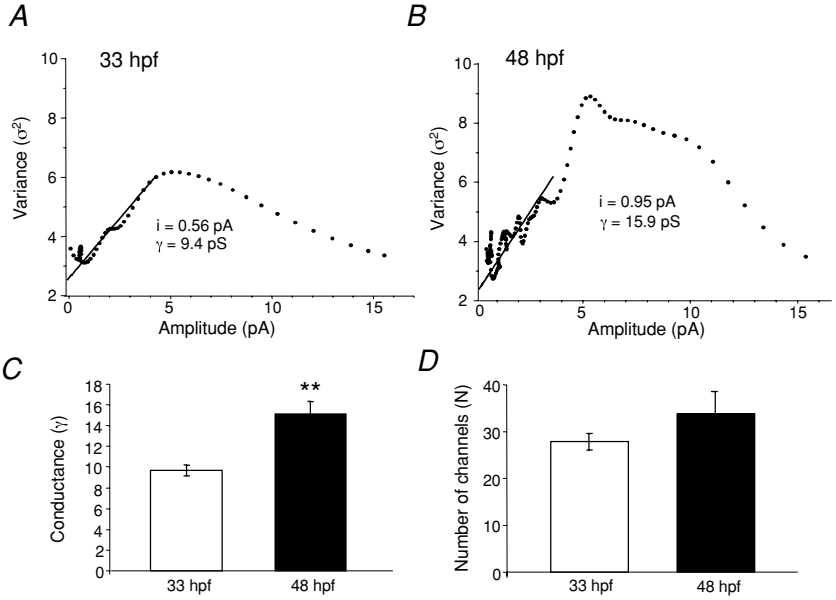

Figure 7. Estimates of synaptic conductance and the number of available AMPARs underlying mEPSCs
A, plot of variance *versus* mean current amplitude of mEPSCs at 33 hpf. *B*, plot of variance *versus* mean current amplitude of mEPSCs at 48 hpf. The line (*A* and *B*) indicates the fit of the initial portion of the plot to the theoretical equation (see Methods) and it gives an estimate of the elementary current (*i*) generated by the activation of one receptor. The conductance (γ) was calculated from the equation. $\gamma = i/V_H$ ($V_H = -60$ mV). In the experiments shown, $\gamma = 9.4$ pS at 33 hpf and 15.9 pS at 48 hpf. *C*, bar graph of the conductance at 33 hpf (9.6 ± 0.5, $n = 5$ embryos) and 48 hpf (15.2 ± 1.2, $n = 6$ larvae). *D*, bar graph of the number of the available AMPARs, *N*, at 33 hpf (27 ± 2) and 48 hpf (33 ± 5). *Significance at $P < 0.05$ and ** at $P < 0.01$.

AMPAR-mediated mEPSCs are not due to alterations in the glutamate transients in the synaptic cleft, which may be indicative of changes in synaptic morphology, but rather, may not be due to a switch in AMPAR subunits.

Here, we provide several lines of evidence that are consistent with a switch in AMPAR subunits. First, application of DL-TBOA and KYN did not alter the kinetics of the mEPSC, suggesting that glutamate uptake or the glutamate concentration in the synaptic cleft did not change during development. Second, the decay time course of AMPAR mEPSCs decreases between 33 hpf and 48 hpf. Third, in 48 hpf fish, the decay time constant is affected

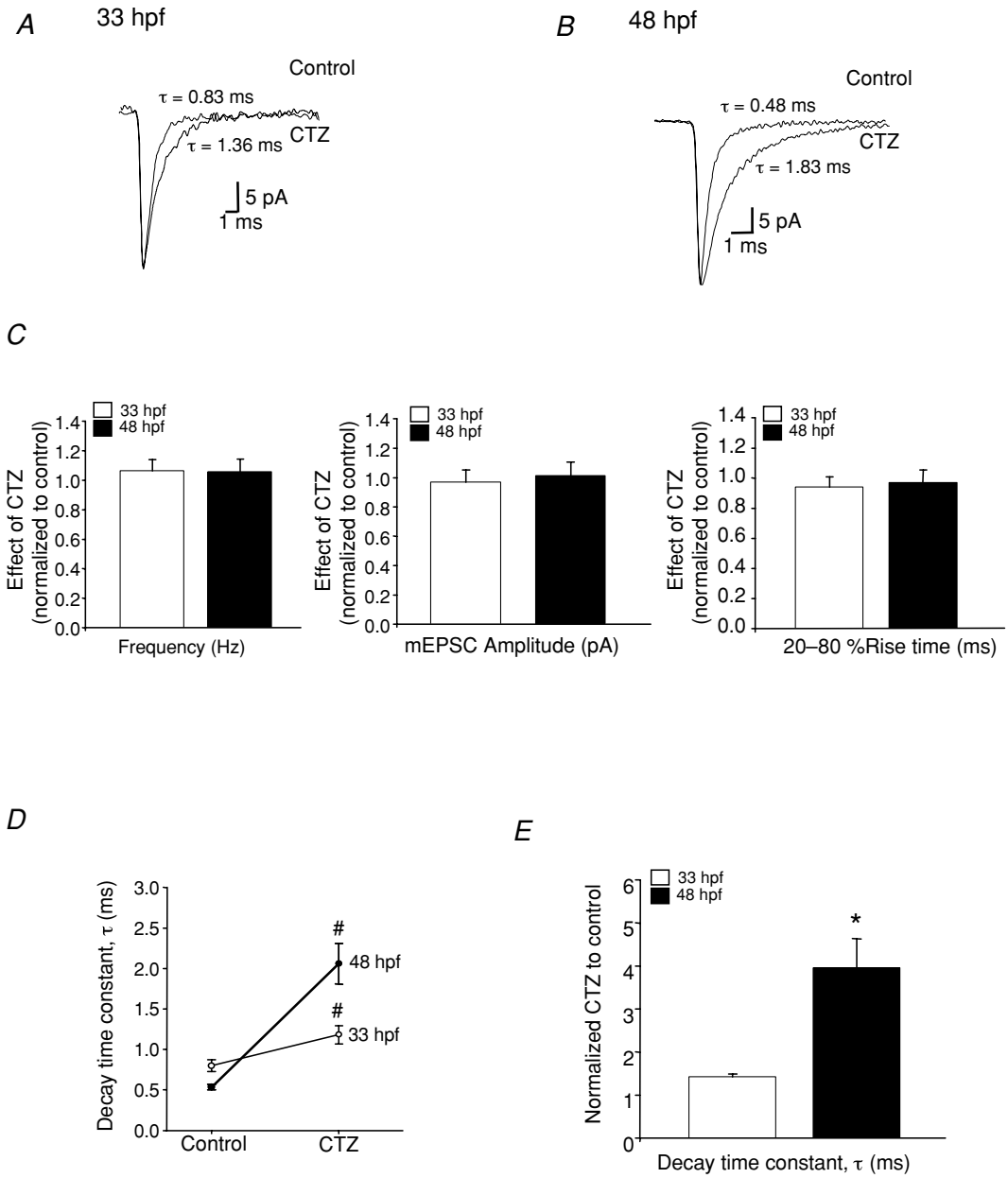

Figure 8. Effects of CTZ on AMPAR-mEPSCs
A, average mEPSCs recorded from 33 hpf M-cells in the absence (control) and presence of 10 μM CTZ ($n = 3$ embryos, $V_H = -60$ mV). *B*, average mEPSCs recorded from 48 hpf M-cells in the absence (control) and presence of 10 μM CTZ ($n = 4$ larvae). Events recorded in the presence of CTZ were normalized to their controls recorded in the absence of CTZ. *C*, bar graphs showing the effect of CTZ on the frequency, peak amplitude and 20–80% rise time at 33 hpf (open bars) and 48 hpf (filled bars). *D*, the decay time constant (τ) of averaged mEPSCs at 33 hpf and 48 hpf in the presence of 10 μm CTZ. *E*, bar graph showing τ of mEPSCs recorded in 10 μm CTZ normalized to control mEPSCs recorded in the absence of CTZ, illustrating the effect of CTZ on the decay time constant of the mEPSCs at 33 hpf and 48 hpf. *Significantly different from the age group 33 hpf, $P < 0.05$; #significantly different from control $P < 0.05$.

by voltage to a much larger degree than it is at 33 hpf. Fourth, CTZ increases the decay time constant of AMPAR mEPSCs 4-fold in 48 hpf fish, but only 1.5-fold at 33 hpf, and fifth, the main single-channel conductance of AMPAR at 33 hpf is ∼9 pS, but ∼15 pS at 48 hpf. Taken together, these data suggest that the population of AMPARs at 33 hpf is likely to be functionally different from that at 48 hpf.

Our results show that the time course of AMPAR mEPSCs became faster during development. The decay kinetics of AMPAR-EPSCs can be influenced by a number of factors, including the composition of the postsynaptic receptors (Edmonds *et al.* 1995; Conti & Weinberg, 1999), the rate at which they desensitize (Jones & Westbrook, 1996), the dynamics of glutamate in the synaptic cleft (e.g. release, clearance), and changes in synaptic structure and the surrounding neuropil (Cathala *et al.* 2005). Our findings are similar to a number of other studies, which show a developmental speeding of AMPA mEPSC kinetics in preparations such as the rat cochlear nucleus (Brenowitz & Trussell, 2001), cerebellar mossy fibre granule cells (Wall *et al.* 2002), median nucleus trapezoid bodies (Taschenberger & von Gersdorff, 2000) and mammalian neocortical pyramidal neurons (Kumar *et al.* 2002). These changes are thought to occur due to alterations in the composition of the AMPA receptor (Edmonds *et al.* 1995; Conti & Weinberg, 1999; Kumar *et al.* 2002). Similarly, a switch in receptor subunit composition is thought to underlie the developmental speeding of the decay time course in glycinergic and NMDA receptor-mediated synaptic currents (Hestrin, 1992; Takahashi *et al.* 1996; Singer *et al.* 1998). However, a recent study has shown that the speeding of AMPA EPSC kinetics in mouse cerebellar granule cells occurs via a different mechanism: maturation of synaptic morphology rather than subunit alterations (Cathala *et al.* 2005). Our findings suggest that in zebrafish M-cells, subunit switching is likely to be the main determinant of the accelerated decay of AMPAR-EPSCs.

The decay time constant increased with depolarization at all ages, but this occurred to a greater extent in older animals. A similar voltage-dependent effect on the AMPA mEPSC decay kinetics has been reported (Otis *et al.* 1996; Glowatzki & Fuchs, 2002; Morkve *et al.* 2002); however, it is not known which subunit(s) might be responsible for this property (Morkve *et al.* 2002). We observed a significant difference in the percentage increase in the decay time constant with depolarization between 33 hpf and 48 hpf animals, suggesting that the receptor gating properties contributing to the EPSC decay kinetics are different at those ages. Since receptor gating properties are dependent on the receptor's subunit composition, it is likely that the AMPARs in M-cells undergo a developmental switch in their subunit composition.

One of our most compelling findings was the differential effect of CTZ at 48 hpf compared with 33 hpf. We were careful to use low concentrations of CTZ in order to ensure specificity (Partin *et al.* 1994; Cathala *et al.* 2005) on AMPARs. The dramatic increase in τ at 48 hpf, but not at 33 hpf, suggests that the alternatively spliced, flip variant may be present in greater quantities in older animals. CTZ blocks desensitization of AMPARs and preferentially has a stronger effect on the flip forms of the subunits (Partin *et al.* 1994). Thus the differential effects of CTZ at 48 hpf and 33 hpf argue in favour of the flop form associated with M-cells early in development, with the emerging onset of the flip version sometime later. This contrasts with a recent study showing that the flip form of GluR2 is the predominant form in the CNS at 30 hpf (Lin *et al.* 2006). Interestingly, while both forms increase in expression after 30 hpf, the flip variant is expressed in greater amounts (Lin *et al.* 2006). Finally, since CTZ is thought to have a greater degree of potentiation on homomeric receptors (Cotton & Partin, 2000), our results indicate that the AMPARs at 33 hpf may be heteromeric, while those at 48 hpf are likely to be homomeric. However, it should be noted that the differential effect of CTZ at the different ages may also be due to unknown developmental changes occurring within the synapse. For instance, if the receptors desensitize differently due to differential phosphorylation mechanisms, then the responses to CTZ may be different between the two ages.

We found that in older animals (48 hpf to 72 hpf), the AMPARs exhibited outward rectification, while at 33 hpf the relationship was linear. This was a curious finding because most AMPA receptors exhibit either a linear or inward rectification (Verdoorn *et al.* 1991; Koh *et al.* 1995; Lui & Cull-Candy 2000). However, some GluR2-containing receptors do display outward rectification in the edited form (Verdoorn *et al.* 1991; Morkve *et al.* 2002). The fact that we detected only a linear *I–V* relation in the young animals, and only outward rectification in older fish, supports our view that the AMPA receptors are different between the two ages. Site-directed mutagenesis of single amino acid residues of AMPAR subunits may cause outward rectification (Dingledine *et al.* 1992). Our findings suggest that the amino acid identity of AMPARs in zebrafish is most certainly different from that in mammals, and may underlie some of the interesting properties that we have seen.

The small but significant developmental increase in mEPSC amplitude could be due to a number of factors, including an increase in (1) the number of postsynaptic receptors; (2) single-channel conductance; (3) quantal content; or (4) a change in synaptic morphology. AMPARs on 33 hpf M-cells exhibited a smaller conductance (∼9 pS) than those at 48 hpf (∼15 pS). Our findings are similar to those observed in other systems where values of ∼8–10 pS and 15–20 pS have been found (Morkve *et al.* 2002;

Momiyama *et al.* 2003; Bannister *et al.* 2005; Cathala *et al.* 2005). The conductance of AMPARs is critically dependent upon subunit composition (Swanson *et al.* 1997), suggesting that the different conductances we have seen at 33 hpf and 48 hpf are due to separate populations at these two ages. What might be the physiological significance of a subunit switch? Current theory suggests that a speeding in AMPAR kinetics occurs in order to ensure temporal precision and increased efficiency of information transfer (London *et al.* 2002). In zebrafish, the switch in subunits occurs between 33 h and 48 h, immediately prior to hatching at 48–52 hpf. The perceived advantage would be increased efficiency in the escape response that is necessary for survival.

In summary, we have characterized a number of developmental changes in AMPAR-mediated synaptic currents in Mauthner neurons. Our findings are similar to those of previous reports that show a developmental change in the composition of AMPARs (Bellingham *et al.* 1998; Taschenberger & von Gersdorff, 2000; Kumar *et al.* 2002; Wall *et al.* 2002). While our results suggest that a subunit switch occurs, they are not conclusive, and it is possible that unknown developmental mechanisms may account for a number of the changes that we have seen. Our findings indicate that the AMPARs at the ages examined contain at least one GluR2 subunit, and that the overall receptor subunit assembly probably changes between 33 hpf and 48 hpf. All of these changes occur between 33 hpf and 48 hpf, which is a critical period for synapse formation (Kimmel *et al.* 1981), sensory onset (Eaton & Farley, 1973) and morphological maturation of the M-cell (Kimmel *et al.* 1981).

References

Ali DW, Buss RR & Drapeau P (2000*a*). Properties of miniature glutamatergic EPSCs in neurons of the locomotor regions of the developing zebrafish. *J Neurophysiol* **83**, 181–191.

Ali DW, Drapeau P & Legendre P (2000*b*). Development of spontaneous glycinergic currents in the Mauthner neuron of the zebrafish embryo. *J Neurophysiol* **84**, 1726–1736.

Ambros-Ingerson J & Lynch G (1993). Channel gating kinetics and synaptic efficacy: a hypothesis for expression of long-term potentiation. *Proc Natl Acad Sci U S A* **90**, 7903–7907.

Bannister NJ, Benke TA, Mellor J, Scott H, Gurdal E, Crabtree JW & Isaac JT (2005). Developmental changes in AMPA and kainate receptor-mediated quantal transmission at thalamocortical synapses in the barrel cortex. *J Neurosci* **25**, 5259–5271.

Bellingham MC, Lim R & Walmsley B (1998). Developmental changes in EPSC quantal size and quantal content at a central glutamatergic synapse in rat. *J Physiol* **511**, 861–869.

Benke TA, Luthi A, Isaac JTR & Collingridge GL (1998). Modulation of AMPA receptor unitary conductance by synaptic activity. *Nature* **395**, 793–797.

Benke TA, Luthi A, Palmer MJ, Wikstrom MA, Anderson WW, Isaac JT & Collingridge GL (2001). Mathematical modelling of non-stationary fluctuation analysis for studying channel properties of synaptic AMPA receptors. *J Physiol* **537**, 407–420.

Brenowitz S & Trussell LO (2001). Maturation of synaptic transmission at end-bulb synapses of the cochlear nucleus. *J Neurosci* **21**, 9487–9498.

Cathala L, Brickley S, Cull-Candy S & Farrant M (2003). Maturation of EPSCs and intrinsic membrane properties enhances precision at a cerebellar synapse. *J Neurosci* **23**, 6074–6085.

Cathala L, Holderith NB, Nusser Z, DiGregorio DA & Cull-Candy SG (2005). Changes in synaptic structure underlie the developmental speeding of AMPA receptor-mediated EPSCs. *Nat Neurosci* **8**, 1310–1318.

Clements JD & Westbrook GL (1991). Activation kinetics reveal the number of glutamate and glycine binding sites on the *N*-methyl-D-aspartate receptor. *Neuron* **7**, 605–613.

Conti F & Weinberg RJ (1999). Shaping excitation at glutamatergic synapses. *Trends Neurosci* **22**, 451–458.

Cotton JL & Partin KM (2000). The contributions of GluR2 to allosteric modulation of AMPA receptors. *Neuropharmacology* **39**, 21–31.

Cull-Candy S, Kelly L & Farrant M (2006). Regulation of Ca^{2+}-permeable AMPA receptors: synaptic plasticity and beyond. *Curr Opin Neurobiol* **16**, 288–297.

Diamond JS & Jahr CE (1997). Transporters buffer synaptically released glutamate on a submillisecond time scale. *J Neurosci* **17**, 4672–4687.

Dingledine R, Hume RI & Heinemann SF (1992). Structural determinants of barium permeation and rectification in non-NMDA glutamate receptor channels. *J Neurosci* **12**, 4080–4087.

Drapeau P, Ali DW, Buss RR & Saint-Amant L (1999). In vivo recording from identifiable neurons of the locomotor network in the developing zebrafish. *J Neurosci Meth* **88**, 1–13.

Eaton R & Farley RD (1973). Development of the Mauthner neurons in embryos and larvae of the zebrafish, *Brachydanio rerio*. *Copeia* **4**, 673–682.

Edmonds B, Gibb AJ & Colquhoun D (1995). Mechanisms of activation of glutamate receptors and the time course of excitatory synaptic currents. *Annu Rev Physiol* **57**, 495–519.

Evans DH (1979). Fish. In *Comparative Physiolology of Osmoregulation in Animals* Volume l, ed. Maloiy GMO, pp. 305–370. Academic Press, Orlando,

Fetcho JR (2006). The utility of zebrafish for studies of the comparative biology of motor systems. *J Exp Zool (Mol Dev Evol)* **306B**, 1–13.

Geiger JR, Melcher T, Koh DS, Sakmann B, Seeburg PH, Jonas P & Monyer H (1995). Relative abundance of subunit mRNAs determines gating and Ca^{2+} permeability of AMPA receptors in principal neurons and interneurons in rat CNS. *Neuron* **15**, 193–204.

Glowatzki E & Fuchs PA (2002). Transmitter release at the hair cell ribbon synapse. *Nat Neurosci* **5**, 147–154.

Grunwald DJ, Kimmel CB, Westerfield M, Walker C & Streisinger G (1988). A neural degeneration mutation that spares primary neurons in the zebrafish. *Dev Biol* **126**, 115–128.

Hestrin S (1992). Developmental regulation of NMDA receptor-mediated synaptic currents at a central synapse. *Nature* **357**, 686–689.

Hollmann M & Heinemann S (1994). Cloned glutamate receptors. *Annu Rev Neurosci* **17**, 31–108.

Iwasaki S & Takahashi T (2001). Developmental regulation of transmitter release at the calyx of Held in rat auditory brainstem. *J Physiol* **534**, 861–871.

Jones MV, Sahara Y, Dzubay JA & Westbrook GL (1998). Defining affinity with the GABAA receptor. *J. Neurosci* **18**, 8590–8604.

Jones MV & Westbrook GL (1996). The impact of receptor desensitization on fast synaptic transmission. *Trends Neurosci* **19**, 96–101.

Joshi I & Wang L-Y (2002). Developmental profiles of glutamate receptors and synaptic transmission at a single synapse in the mouse auditory brainstem. *J Physiol* **540**, 861–873.

Kimmel CB, Ballard WW, Kimmel SR, Ullmann B & Schilling TF (1995). Stages of embryonic development of the zebrafish. *Dev Dyn* **203**, 253–310.

Kimmel CB, Hatta K & Metcalfe WK (1990). Early axonal contacts during development of an identified dendrite in the brain of the zebrafish. *Neuron Apr* **4**, 535–545.

Kimmel CB, Sessions SK & Kimmel RJ (1981). Morphogenesis and synaptogenesis of the zebrafish Mauthner neuron. *J Comp Neurol* **198**, 101–120.

Koh DS, Burnashev N & Jonas P (1995). Block of native Ca^{2+}-permeable AMPA receptors in rat brain by intracellular polyamines generates double rectification. *J Physiol* **486**, 305–312. Erratum in *J Physiol* **488**, 843.

Kumar SS, Bacci A, Kharazia V & Huguenard JR (2002). A developmental switch of AMPA receptor subunits in neocortical pyramidal neurons. *J Neurosci* **22**, 3005–3015.

Lawrence JJ & Trussell LO (2000). Long-term specification of AMPA receptor properties after synapse formation. *J Neurosci* **20**, 4864–4870.

Lee SH & Sheng M (2000). Development of neuron-neuron synapses. *Curr Opin Neurobiol* **15**, 125–131.

Legendre P (1998). A reluctant gating mode of glycine receptor channels determines the time course of inhibitory miniature synaptic events in zebrafiah hindbrain neurons. *J. Neurosci* **18**, 2856–2870.

Lin B, Brucher FA, Colgin LL & Lynch G (2002). Long-term potentiation alters the modulator pharmacology of AMPA-type glutamate receptors. *J Neurophysiol* **87**, 2790–2800.

Lin WH, Wu CH, Chen YC & Chow WY (2006). Embryonic expression of zebrafish AMPA receptor genes: Zygotic gria2alpha expression initiates at the midblastula transition. *Brain Res* **1110**, 46–54.

Liu SJ & Cull-Candy SG (2002). Activity-dependent change in AMPA receptor properties in cerebellar stellate cells. *J Neurosci* **22**, 3881–3889.

Liu KS & Fetcho JR (1999). Laser ablations reveal functional relationships of segmental hindbrain neurons in. Zebrafish. *Neuron* **23**, 325–335.

London M, Schreibman A, Hausser M, Larkum ME & Segev I (2002). The information efficacy of a synapse. *Nat Neurosci* **5**, 332–340.

Metcalfe WK, Myers PZ, Trevarrow B, Bass MB & Kimmel CB (1990). Primary neurons that express the L2/HNK-1 carbohydrate during early development in the zebrafish. *Development* **110**, 491–504.

Momiyama A, Silver RA, Hausser M, Notomi T, Wu Y, Shigemoto R & Cull-Candy SG (2003). The density of AMPA receptors activated by a transmitter quantum at the climbing fibre-Purkinje cell synapse in immature rats. *J Physiol* **549**, 75–92.

Morkve SH, Veruki ML & Hartveit E (2002). Functional characteristics of non-NMDA-type ionotropic glutamate receptor channels in AII amacrine cells in rat retina. *J Physiol* **542**, 147–165.

Otis TS, Raman IM & Trussell LO (1995). AMPA receptors with high Ca^{2+} permeability mediate synaptic transmission in the avian auditory pathway. *J Physiol* **482**, 309–315.

Otis T, Zhang S & Trussell LO (1996). Direct measurement of AMPA receptor desensitization induced by glutamatergic synaptictransmission. *J Neurosci* **16**, 7496–7504.

Partin KM, Bowie D & Mayer ML (1995). Structural determinants of allosteric regulation in alternatively spliced AMPA receptors. *Neuron* **14**, 833–843.

Partin KM, Patneau DK & Mayer ML (1994). Cyclothiazide differentially modulates desensitization of alpha-amino-3-hydroxy-5-methyl-4-isoxazolepropionic acid receptor splice variants. *Mol Pharmacol* **46**, 129–138.

Partin KM, Patneau DK, Winters CA, Mayer ML & Buonanno A (1993). Selective modulation of desensitization at AMPA versus kainate receptors by cyclothiazide and concanavalin A. *Neuron* **11**, 1069–1082.

Rall W (1969). Time constants and electrotonic length of membrane cylinders and neurons. *Biophys J* **9**, 1483–1508.

Rumpel S, Kattenstroth G & Gottmann K (2004). Silent synapses in the immature visual cortex: layer-specific developmental regulation. *J Neurophysiol* **91**, 1097–1101.

Sah P & Lopez De Armentia M (2003). Excitatory synaptic transmission in the lateral and central amygdala. *Ann N Y Acad Sci* **985**, 67–77.

Sakmann B & Brenner HR (1978). Change in synaptic channel gating during neuromuscular development. *Nature* **276**, 401–402.

Schmitt WB, Arianpour R, Deacon RM, Seeburg PH, Sprengel R, Rawlins JN & Bannerman DM (2004). The role of hippocampal glutamate receptor-A-dependent synaptic plasticity in conditional learning: the importance of spatiotemporal discontiguity. *J Neurosci* **24**, 7277–7282.

Seeburg PH (1996). The role of RNA editing in controlling glutamate receptor channel properties. *J Neurochem* **66**, 1–5.

Seifert G, Zhou M, Dietrich D, Schumacher TB, Dybek A, Weiser T, Wienrich M, Wilhelm D & Steinhauser C (2000). Developmental regulation of AMPA-receptor properties in CA1 pyramidal neurons of rat hippocampus. *Neuropharmacol* **39**, 931–942.

Sigworth FJ (1980). The variance of sodium current fluctuations at the node of Ranvier. *J Physiol* **307**, 97–129.

Silver RA, Cull-Candy SG & Takahashi T (1996). Non-NMDA glutamate receptor occupancy and open probability at a rat cerebellar synapse with single and multiple release sites. *J Physiol* **494**, 231–250.

Singer JH, Talley EM, Bayliss DA & Berger AJ (1998). Development of glycinergic synaptic transmission to rat brain stem motoneurons. *J Neurophysiol* **80**, 2608–2620.

Sommer B, Keinanen K, Verdoorn TA, Wisden W, Burnashev N, Herb A, Kohler M, Takagi T, Sakmann B & Seeburg PH (1990). Flip and flop: a cell-specific functional switch in glutamate-operated channels of the CNS. *Science* **249**, 1580–1585.

Swanson GT, Kamboj SK & Cull-Candy SG (1997). Single-channel properties of recombinant AMPA receptors depend on RNA editing, splice variation, and subunit composition. *J Neurosci* **17**, 58–69.

Takahashi T, Feldmeyer D, Suzuki N, Onodera K, Cull-Candy SG, Sakimura K & Mishina M (1996). Functional correlation of NMDA receptor epsilon subunits expression with the properties of single-channel and synaptic currents in the developing cerebellum. *J Neurosci* **16,** 4376–4382.

Taschenberger H & von Gersdorff H (2000). Fine-tuning an auditory synapse for speed and fidelity: developmental changes in presynaptic waveform, EPSC kinetics, and synaptic plasticity. *J Neurosci* **20**, 9162–9173.

Traynelis SF, Silver RA & Cull-Candy SG (1993). Estimated conductance of glutamate receptor channels activated during EPSCs at the cerebellar mossy fiber-granule cell synapse. *Neuron* **11**, 279–289.

Vaithianathan T, Matthias K, Bahr B, Schachner M, Suppiramaniam V, Dityatev A & Steinhauser C (2004). Neural cell adhesion molecule-associated polysialic acid potentiates alpha-amino-3-hydroxy-5-methylisoxazole-4-propionic acid receptor currents. *J Biol Chem* **279**, 47975–47984.

Verdoorn TA, Burnashev N, Monyer H, Seeburg PH & Sakmann B (1991). Structural determinants of ion flow through recombinant glutamate receptor channels. *Science* **252**, 1715–1718.

Wadiche JI & Jahr CE (2001). Multivesicular release at climbing fiber–Purkinje cell synapses. *Neuron* **32**, 301–313.

Wall MJ, Robert A, Howe JR & Usowicz MM (2002). The speeding of EPSC kinetics during maturation of a central synapse. *Eur J Neurosci* **15**, 785–797.

Westerfield M (2000). *The Zebrafish Book. A Guide for the Laboratory Use of Zebrafish* (Danio rerio), 4th edn. University of Oregon Press, Eugene.

Wong LA & Mayer ML (1993). Differential modulation by cyclothiazide and concanavalin A of desensitization at native alpha-amino-3-hydroxy-5-methyl-4-isoxazolepropionic acid- and kainate-preferring glutamate receptors. *Mol Pharmacol* **44**, 504–510.

Yamashita T, Ishikawa T & Takahashi T (2003). Developmental increase in vesicular glutamate content dose not cause saturation of AMPA receptors at the calyx of Held synapse. *J Neurosci* **23**, 3633–3638.

Acknowledgements

This work was supported by grants from the Natural Sciences and Engineering Research Council of Canada (NSERC) and the Canadian Foundation for Innovation (CFI) to DWA. The authors wish to thank Dr Pascal Legendre for helpful instructions regarding the non-stationary fluctuation analysis (NSFA).

Supplemental material

Online supplemental material for this paper can be accessed at:
http://jp.physoc.org/cgi/content/full/jphysiol.2007.129999/DC1
and
http://www.blackwell-synergy.com/doi/suppl/10.1113/jphysiol.2007.129999